Asphalt Flocculation and Deposition: II. Formation and Growth of Fractal Aggregates

Hossein Rassamdana and Muhammad Sahimi
Dept. of Chemical Engineering, University of Southern California, Los Angeles, CA 90089

Extensive small-angle X-ray and neutron-scattering data, as well as results of precipitation measurements, are analyzed to delineate the structure of the asphalt and asphaltene aggregates that are formed when a solvent is injected into a system containing crude oil. The two types of data strongly suggest that both small and large aggregates have a fractal structure, with well-defined fractal dimensions. If the system is aged long enough at low enough temperature, large asphalt particles will have the structure of diffusion-limited cluster–cluster aggregates with a fractal dimension $D_f \simeq 1.8$, while the small ones are similar to diffusion-limited particle aggregates with a fractal dimension $d_f \simeq 2.5$. High temperatures increase the rotational motion of the particles, disturb the structure and mechanical stability of the aggregates, and decrease their fractal dimension. Aging and concentration effects of the asphalts in the solution, and the type of the solvent on the structure of the aggregates are also investigated. Implications of these results for the structure, mechanical stability, and molecular-weight distribution of asphalts and asphaltenes are detailed. A new molecular-weight distribution for asphalt aggregates predicts the experimental data excellently.

Introduction

Formation, flow and precipitation of particles or large aggregates in porous media are relevant to a wide variety of natural and industrial processes, such as deep-bed filtration, flow of dilute stable emulsions, migration of fines, and catalysis (for a review, see Sahimi et al., 1990), as well as groundwater contamination and enhanced oil recovery (for reviews, see Sahimi, 1993, 1995). The efficiency of these processes depends crucially on the availability of open-pore space, which provides transport paths for the fluid that carries the aggregates. In some cases, the particles or aggregates are formed when the fluid in the porous medium reacts with the solid matrix, resulting in solid products that are carried away by the flowing fluid. In other cases, the aggregates are formed when a fluid is injected into the pore space to react with, or displace, the in-place fluid. These aggregates have very unusual properties, and despite many years of research a definitive model of their structure has not emerged.

Consider a typical process in which such aggregates are formed, namely, catalytic coal liquefaction and coal liquid upgrading, during which large molecular aggregates, that are usually referred to as asphaltene, are formed, whose precipitation on the pore surfaces of the catalyst decreases severely the efficiency of these processes. Over the years several studies have been undertaken (see, for example, Thrash and Pildes, 1981; Baltus and Anderson, 1983; Sakai et al., 1983; Mieville et al., 1989; Kyriacou et al., 1988a,b; Nortz et al., 1990; Sane et al., 1988, 1992) by which the transport properties of asphaltenes derived from various types of heavy oil have been measured. However, in the absence of a reasonable structural model of the asphaltenes, such data cannot be interpreted and correlated accurately. Moreover, precipitation of the asphaltene aggregates on the pore surfaces of the catalyst causes severe problems for efficient operation of the process, and thus one also needs an accurate model for predicting the precipitation and its onset, at which it is triggered. Despite some recent progress (see below), a generally accepted model has not emerged yet.

Consider another industrial process in which such aggregates are formed, namely, enhanced oil recovery from an underground reservoir by a miscible displacement process in which an agent—a gas or a liquid—is injected into the reser-

Correspondence concerning this article should be addressed to M. Sahimi.
Additional address for H. Rassamdana: Improved Oil Recovery Center, National Iranian Oil Company, Teleghani Avenue, Tehran, Iran.

voir to displace the oil. This often causes formation of large asphalt or asphaltene aggregates consisting of heavy organic compounds and their precipitation on the pore surfaces of the reservoir during the enhanced oil-recovery process (Speight, 1991). For the sake of clarity we define (as do others; see, e.g., Speight, 1991) asphalts as asphaltenes plus resin and wax. Formation of asphalt and asphaltene aggregates is a function of the composition of the crude oil and the displacing agents, and the pressure and temperature of the reservoir. Their deposition on the surface of the pores reduces the permeability of the pore space, leading to the eventual isolation of oil from the flowing fluid in the reservoir (see, for example, Lichaa and Herrera, 1975), a reduction in the efficiency of oil recovery processes, and an increase in their cost. Therefore, it is important to understand the mechanisms of formation of such aggregates under the reservoir conditions, the point at which their deposition on the pore surfaces is triggered, their thermodynamic and transport properties, and their effect on the properties of the pore space. Although over the past several decades such problems have been studied intensively (see, for example, Yen, 1990, and Speight, 1991, for comprehensive reviews), no general consensus has emerged.

In a previous article (Rassamdana et al., 1996, hereafter referred to as Part I), we presented the results of a systematic study of asphalt formation near the onset of precipitation, which is particularly important to oil recovery, reported new experimental data for the amount of the precipitates, and presented two theoretical approaches for predicting them. In the present article we study the kinetic growth of asphalt and asphaltene aggregates. We analyze two completely different classes of experimental data. One is our precipitation data reported in Part I, which we analyze in order to gain insight into the structure of the asphalt aggregates. Small-angle scattering measurements, a highly accurate probe of the structure of molecular aggregates, constitute the second class of data that we analyze. We show that both types of data lead us to an unambiguous and novel model of the structure of the asphalt aggregates. The model has important implications for several structural and dynamical properties of the aggregates, which we discuss in detail. Effective diffusivities of asphalt aggregates in a pore have been reported elsewhere (Ravi-Kumar et al., 1994).

The plan of this article is as follows. In the next section we describe two models of formation and kinetic growth of molecular aggregates that are relevant to our discussion. We then describe the theory of small-angle scattering by fractal aggregates. Next, extensive small-angle X-ray and neutron scattering (SAXS and SANS, respectively) data are analyzed and are shown to be consistent with a fractal structure for the asphalt and asphaltene aggregates. The effects of the various factors that affect the structure of the aggregates, such as the temperature of the system and the composition of the crude oil and the solvent are discussed in detail. In the next section, we analyze precipitation data and show that they are consistent with the scattering results, thus lending strong support to the fractality of the asphalt and asphaltene aggregates. We then discuss the implications of these results, including those for modeling aggregation of asphalts, their stability against temperature fluctuations, and their molecular weight distribution.

Particle and Cluster Aggregation

Two important aggregation processes that are relevant to our article are diffusion-limited particle (DLP) and diffusion-limited cluster–cluster (DLCC) aggregation (see Meakin, 1988, for an excellent review). Here, we summarize briefly those aspects of these processes that are directly relevant to our discussion. In the DLP aggregation model (Witten and Sander, 1981), the site at the center of a lattice is occupied by a stationary particle. A particle is then injected into the lattice, far from the center, that diffuses (executes a random walk) on the lattice. If it reaches a surface site, that is, an empty site that is a nearest neighbor to the stationary particle, it sticks to that site and remains there permanently. Another particle is then injected into the lattice, which diffuses on the lattice until it reaches another surface (empty) site and sticks to it, and so on. If the process is continued for a long time, a large aggregate is formed, a typical 2-D example of which is shown in Figure 1. The DLP aggregates are self-similar and fractal, that is, if their radius is R_p and they contain N_p elementary particles, then

$$N_p \sim R_p^{D_f}, \tag{1}$$

where D_f is their fractal dimension. Computer simulations (Meakin, 1988) indicate that $D_f \simeq 1.7$ and 2.5, for 2-D and 3-D DLP aggregates, respectively.

In the DLCC aggregation model (Meakin, 1983; Kolb et al., 1983), one starts with an empty lattice. At time $t = 0$, lattice sites are selected at random and occupied by particles, until a small fraction p_0 of the sites are occupied by the particles. Each occupied site can contain only one particle. A randomly selected cluster of occupied sites, including a single site, is then selected and moved (allowed to diffuse) in a randomly chosen direction. Then the perimeter sites of the cluster—the set of sites that is adjacent to the cluster—are ex-

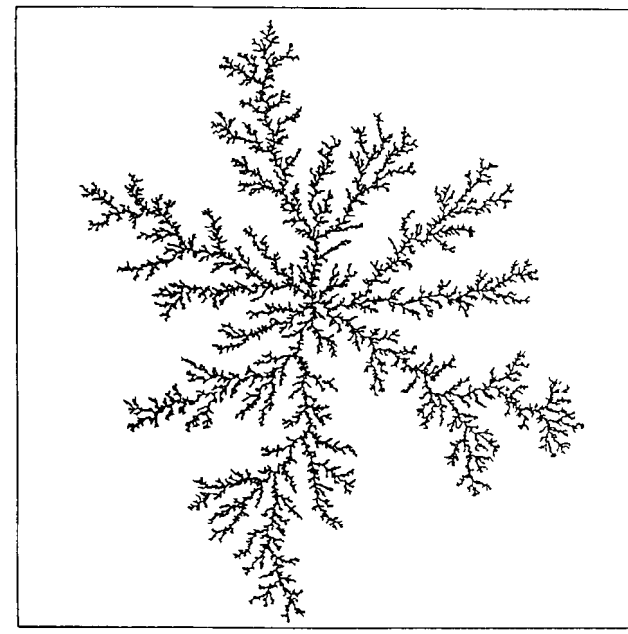

Figure 1. Two-dimensional diffusion-limited particle aggregate.

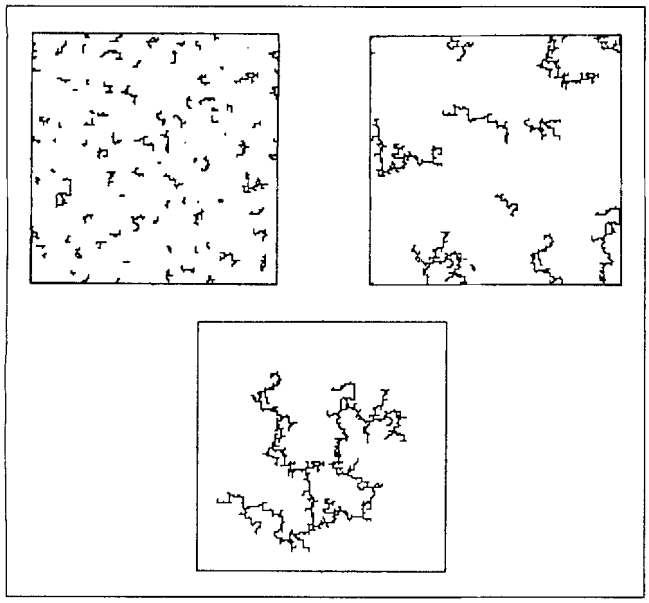

Figure 2. Various stages of formation of a 2-D diffusion-limited cluster–cluster aggregate.

amined to see whether they are occupied by other particles or clusters. If so, the perimeter particles or clusters are added (attached) to the cluster that was moved to form a larger cluster. Once a large cluster is formed, it is not allowed to break up again. (Later in this article we investigate the stability of these aggregates, and the conditions under which the clusters may break up.) Another randomly selected cluster is moved again, its perimeter is examined for possible formation of a larger cluster, and so on. Figure 2 shows three stages of this process in 2-D. Similar to the DLP aggregates, the DLCC aggregates are also fractal objects with $D_f \simeq 1.45 \pm 0.05$ and 1.8 ± 0.05 in 2-D and 3-D, respectively. Observe that the fractal dimension of the DLCC aggregates is smaller than that of the DLP aggregates. The reason for this is clear: aggregation of clusters creates larger holes in the final molecular structure than that of elementary particles. This is clearly seen in Figures 1 and 2. Note that, in this model it is assumed that the diffusivity $\mathfrak{D}$ of a cluster is independent of its molecular weight M. In practice, one expects to have $\mathfrak{D} \sim M^{-1/D_f}$ (since the radius R_p of the cluster is proportional to M^{1/D_f}), or more generally, $\mathfrak{D} \sim M^{\zeta}$, where ζ is an exponent that may depend on the type of solution in which the aggregation takes place. Computer simulations (Meakin, 1988) indicate that D_f is almost completely independent of ζ, provided that $\mathfrak{D}$ decreases with increasing M.

Another important model is the reaction-limited cluster–cluster (RLCC) aggregation process in which the clusters have to touch each other many times before joining. As a result, the clusters can penetrate more deeply into each other, leading to aggregates with a denser structure than that of the DLCC aggregates. For example, their fractal dimension in 3-D is $D_f \simeq 2.05$, compared with $D_f \simeq 1.8$ for DLCC aggregates.

An important property of the DLCC aggregates is their surface roughness. Since the aggregating clusters have irregular shapes and sizes, their *active* surface area S_a, that is, that part of their surface that is most likely to collide with the surface of another cluster, is different from their *total* surface area S, and in fact S_a constitutes only a small fraction of S. The active surface area S_a of an aggregate scales with the total number of particles s in it as

$$S_a \sim s^{\omega}, \tag{2}$$

where ω is a universal exponent, independent of many microscopic features of the aggregate. Obviously, $\omega < 1$, since the active surface area of a cluster cannot grow with its size faster than linearly.

An important property of both the DLCC and RLCC aggregates is their cluster-size distribution. Suppose that $n_s(t)$ is the number of clusters of size s at time t. Then, it has been shown that (Vicsek and Family, 1984)

$$n_s = s^{-\tau} f(s/\langle s \rangle), \tag{3}$$

where τ is a universal exponent, and $\langle s \rangle$ is the mean cluster (aggregate) size defined by

$$\langle s \rangle = \frac{\sum_{s=1}^{\infty} s^2 n_s(t)}{\sum_{s=1}^{\infty} s n_s(t)}. \tag{4}$$

Here $f(x)$ is a *universal* scaling function such that $f(x) \sim x^{\delta}$ for $x \ll 1$ and $f(x) \ll 1$ for $x \gg 1$. For the DLCC aggregates $\tau = 2$ (Vicsek and Family, 1984), while for the RLCC aggregates $\tau = 3/2$ (Ball et al., 1987). Thus, the value of τ can be used to distinguish between the DLCC and RLCC aggregates, which, in fact, is what we do in our analysis of the scattering data discussed below. Obviously, the mean cluster size increases with the time t, and therefore

$$\langle s \rangle \sim t^{w}, \tag{5}$$

where w is a *dynamical* exponent that may depend on ζ, the exponent that relates the diffusivity of the clusters to their molecular weight.

Theory of Small-Angle Scattering by Fractal Aggregates

An accurate probe of the structure of fractal aggregates is small-angle scattering. We define the density–density autocorrelation function $C(r)$ at a distance $r = |\boldsymbol{r}|$ by

$$C(r) = \frac{1}{V} \sum_{r'} g(r') g(r + r'), \tag{6}$$

where V is the volume of the system. The origin of the coordinate system is in the aggregate, $g(r) = 1$ if a given point at a distance r from the origin belongs to the aggregate, and $g(r) = 0$ otherwise. For a d-dimensional self-similar and fractal aggregate of s sites and large values of r we must have

$$C(r) \sim r^{D_f - d}. \tag{7}$$

In a scattering experiment the observed scattering intensity $I_s(\boldsymbol{q})$ by a single cluster is given by the Fourier transform of $C(\boldsymbol{r})$

$$I_s(q) = \int_0^\infty C(r) \exp(iq \cdot r)\, d^3r, \tag{8}$$

where q is the scattering vector whose magnitude q is given by

$$q = \frac{4\pi}{\lambda} \sin\left(\frac{\theta}{2}\right). \tag{9}$$

Here λ is the wavelength of the radiation scattered by the sample through an angle θ. For a system with sufficiently low porosity, such as a fractal aggregate, it is not unreasonable to assume that, to a good approximation, there will be no interference scattering, and therefore the total scattering intensity is the sum of the scattering from all segments of the aggregate. For an isotropic medium, $C(r) = C(r)$, where $r = |r|$, and Eq. 8 becomes

$$I_s(q) = \int_0^\infty 4\pi r^2 \frac{\sin(qr)}{qr} C(r)\, dr. \tag{10}$$

Using Eq. 7 in Eq. 10 with $d = 3$ yields

$$I_s(q) \sim q^{-D_f} \Gamma(D_f - 1) \sin[(D_f - 1)\pi/2], \tag{11}$$

where $\Gamma(x)$ is the gamma function. Thus, a logarithmic plot of the scattering intensity $I_s(q)$ vs. q (or the angle θ) should yield a straight line with the slope $-D_f$. Both light scattering and small-angle X-ray scattering from silica aggregation clusters have confirmed the validity of Eq. 11 (Schaefer et al., 1984). In real systems the range of self-similarity and fractal behavior may be limited by lower and upper cutoff length scales R_l and R_u (see below).

If the solution contains many aggregates or clusters of various sizes, then the intensity $I(q)$ scattered is the average sum of the intensities scattered by all the aggregates. Thus, $I(q)$ is given by (Bouchaud et al., 1986)

$$I(q) = \int s n_s I_s(q)\, ds, \tag{12}$$

which, after using Eqs. 3 and 8, yields

$$I(q) \sim q^{-(3-\tau)D_f}. \tag{13}$$

Note that, since for the DLCC aggregates $\tau = 2$, Eqs. 11 and 13 are identical in this limit. We point out that power-law scattering, such as Eqs. 11 and 13, can also arise from scatterers that are not fractal, but their size distribution is of power-law type. Thus, later in this article we also analyze the precipitation data that provide information about the asphalt cluster-size distribution.

We now analyze the small-angle scattering and precipitation data, from which we attempt to deduce the structure of the asphalt aggregates. We should point out that the small-angle scattering data that we analyze are not ours. However, their presentation and analysis in terms of fractal aggregates is novel and presented for the first time in this article. In the original articles mainly the asphalt particle-size distribution was studied, but no attempt was made to deduce the structure of the aggregates. Moreover, the data that we analyze include both SANS and SAXS, which are known to have very different contrast mechanisms, especially for complex systems such as the asphalt aggregates. Despite this, both types of data lead to the same conclusion regarding the structure of the asphalt aggregates.

Analysis of Small-Angle Scattering Data

We start with the analysis of the SANS data presented by Sheu et al. (1992), and give a brief description of their experiments. The small-angle scattering spectrometer utilizes neutrons from a cold source containing liquid hydrogen at 1.5 K. The outcoming neutrons are monochromatized by a single multilayered monochromator for selection of the wavelength. In the experiments the wavelength was 5.0 Å, with a wavelength spread of about 11%. The sample cell was a cylindrical quartz cuvette of 2-mm path length. The scattered neutrons, after passing through a helium-filled drift space, were detected by a ^{3}He area detector of 50×50 cm^2 containing 128×128 pixel elements. The sample-to-detector distance was 180 cm, which corresponds to a q-range of 0.008 to 0.17 Å^{-1}. Heptane was used as the solvent, and after the aggregates were formed, they were separated from the solution and were mixed with toluene, and the scattering experiments were carried out after 11 days. The aggregate concentration in the toluene ranged from 0.5% to 5% (by weight), with a temperature range of 25° to 43°C.

The logarithmic plot of the scattering intensity $I(q)$ vs. q at 25°C and 5% aggregate concentration is shown as the lower curves in Figure 3. A power-law scattering is observed over about one order of magnitude variation in the length scale. The size of these aggregates appears to be very small, ranging from about 5 Å to about 50 Å. This is due to the fact that in these experiments the asphalt aggregates were dissolved in toluene, which is known to be a good solvent for asphalts and

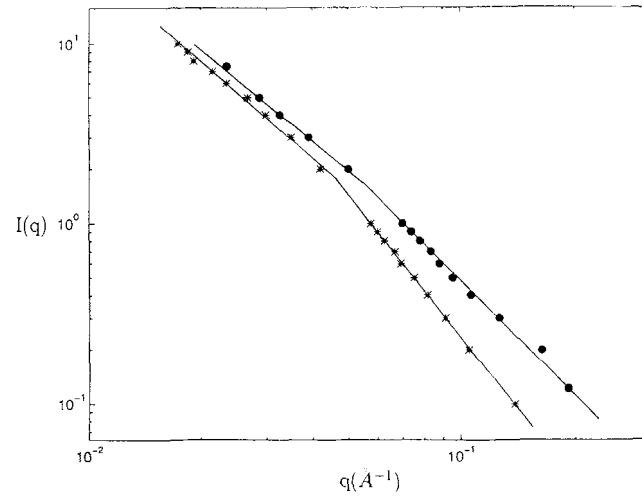

Figure 3. Logarithmic plot of scattering intensity $I(q)$ vs. the magnitude of scattering vector q for the data of Sheu et al. (1992).

The results are for immediately after mixing of the asphalt with toluene (top), and 11 days after the mixing (bottom). The concentration of the asphalt in the solution is 5% at 25°C.

resins and causes fragmentation of the aggregates into small pieces. However, other data analyzed below are for much larger aggregates, and the results are still consistent with what we find from Figure 3. As Figure 3 indicates, there are two distinct regimes. At large length scales (small q) one has a straight line with a slope of about 1.76 ± 0.11, whereas at small length scales (large q), the slope is about 2.6 ± 0.1. Hereafter, we use D_f and d_f to denote the fractal dimensions of the large and small aggregates, respectively. What is the interpretation of these results? From our experimental observations (see Part I) the following mechanism for the formation of the aggregates emerges. After the solvent is added, the resin, that covers the surface of the small individual particles and the self-associates suspended in the oil, is partially dissolved. The particles and the resin are both electrically charged, albeit with opposite signs, and therefore dissolution of the resin creates electrical imbalance between the particles. The small clusters are then formed by diffusion of the charged solid particles in the oil, which stick together upon collision, precisely the way the DLP aggregates are formed. Their fractal dimension, which is about 2.5, is in agreement with the scattering data, $d_f \simeq 2.6 \pm 0.1$, obtained from Figure 3. After some time, one has a mixture of small clusters or aggregates of various sizes (which also carry a net electrical charge), as well as the individual charged particles. So, while the aggregation of the individual particles continues, aggregation of the clusters is also triggered. These clusters and particles also diffuse in the solution and stick to each other upon collision, precisely the mechanism by which the DLCC aggregates are formed. Indeed, with $\tau = 2$, the value for DLCC aggregates, Eq. 13 predicts $D_f \simeq 1.76$ for large length scales, in excellent agreement with that of 3-D DLCC aggregates.

Next, we consider SAXS data reported by Herzog et al. (1988), who used three solution samples. Two of them were oil residues at atmospheric pressure and 350°C. After the solvent, which was n-heptane, was added and the asphalts were formed, they were separated and dispersed in benzene. The third sample was a 10% vacuum residue, containing the asphalt, *without* any separation with n-heptane and dispersed in benzene. The wave length λ was 1.608 Å.

The results presented in Figure 4 show power-law scattering over nearly two orders of magnitude variations in the aggregate size, 50 Å $\leq l \leq$ 1,700 Å. Note that the size of these aggregates is much larger than those in the experiments of Sheu et al. (1992) discussed earlier. The slope for the first two samples is 1.8 ± 0.03, so that if we take $\tau = 2$, the value for the DLCC aggregates, the fractal dimension for the aggregates in the first two samples is $D_f \simeq 1.8 \pm 0.03$, while the third sample yields a fractal dimension $D_f \simeq 1.75 \pm 0.05$, all of which are in excellent agreement with that of 3-D DLCC aggregates, and is also consistent with the SANS data of Sheu et al. (1992), which were for a completely different oil. Note that, the ranges of length scales and the aggregate sizes that have been probed by SAXS in these experiments are much larger than those of Sheu et al.'s, but the results are completely consistent with each other. Note also that, unlike the data of Sheu et al., the results shown in Figure 4 do not indicate the presence in the solution of the DLP aggregates at small length scales. We attribute this to two important factors: one is the aging of the three solutions for a very long time, which provides ample time for the small aggregates to

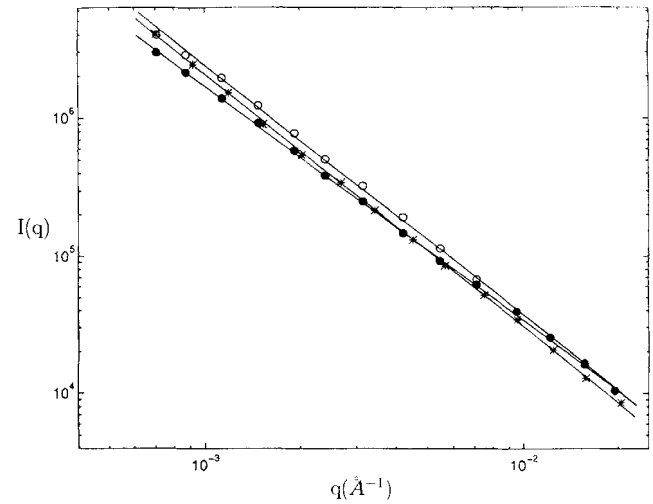

Figure 4. Logarithmic plot of scattering intensity $I(q)$ vs. the magnitude of scattering vector q for the data of Herzog et al. (1988).

The results are for two different oil residues at atmospheric pressure and 350°C (top two), and for a vacuum residue (filled circles).

diffuse in the solution and stick together as they collide. The second factor can be the low concentration of the asphalt in the solution. Most fractal aggregates lose their mechanical stability if their mass exceeds some critical value, and have to restructure themselves (Kantor and Witten, 1984). Thus, if the concentration of the solid particles that constitute the asphalt particles is large enough, initially DLP aggregates are formed, which cluster together later and form a DLCC aggregate. Once the mass of the DLCC aggregate exceeds the critical value, for its mechanical stability, it can no longer absorb the small DLP aggregates, and they are left in the solution. On the other hand, if the concentration is low enough and the system has been aged for a long enough time, it will contain only one type of fractal aggregate. For example, if the asphalt-containing solution is aged for a long enough time, practically all the DLP aggregates as well as the individual charged particles cluster together and form one or more DLCC aggregates. Both of these factors result in virtually no small aggregate left in the solution that can be detected by small-angle scattering.

The next set of SAXS data that we analyze was reported by Dwiggins (1978). In his experiments oil was poured slowly into n-decane (the solvent), being stirred rapidly by a magnetic stirrer in a flask. The resulting solution, which contained 18.6% oil by weight, was then used for SAXS experiments at 25°C. The results are presented in Figure 5. The range of length scales probes in these experiments varies by only a factor of about 4.5, and therefore the results that are inferred from these data cannot by themselves be conclusive. But the size of the aggregates is very large, ranging from about 1,600 Å to about 7200 Å. Moreover, similar to the SANS data of Sheu et al. (1992), they indicate the existence of two distinct regimes. At large length scales (small q) the slope of the line is 1.85 ± 0.1, which together with $\tau = 2$ yield $D_f \simeq 1.85 \pm 0.1$, in agreement with the fractal dimension of the DLCC aggregates, whereas at small length scales (large q) we obtain

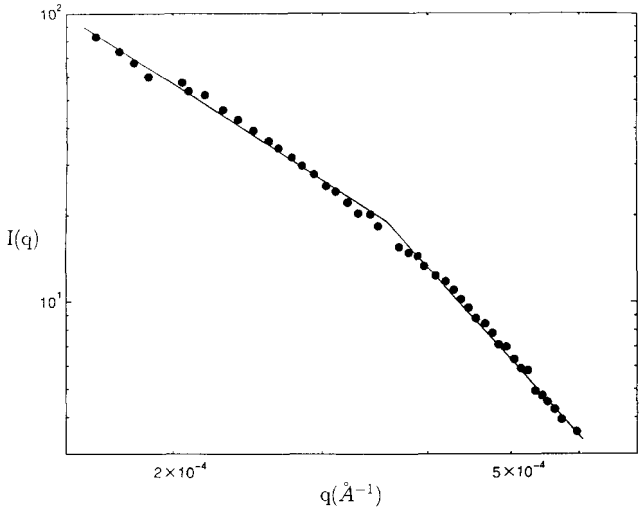

Figure 5. Logarithmic plot of scattering intensity $I(q)$ vs. the magnitude of scattering vector q for the data of Dwinggins (1978).

$d_f \simeq 3$. This value of D_f is again in agreement with that of 3-D DLCC aggregates. However, $d_f \simeq 3$ implies small compact aggregates, for which we have no explanation. Dwiggins (1978) also reported SAXS data for a whole (blank) oil, which is an oil to which no solvent has been added. The results for this solution are shown as the upper curve in Figure 6, which indicates that, over nearly one order of magnitude variations in the length scales, one only has large aggregates with $D_f \simeq 1.87 \pm 0.09$, if we take $\tau = 2$, again in excellent agreement with that of 3-D DLCC aggregates. Dwiggins (1978) himself remarked that, "The curve for the whole oil further indicates the presence of very large particles," consistent with our assertion.

We point out that, if in interpreting the preceding results, we take $\tau = 3/2$, the value for the RLCC aggregates, all the scattering results for large length scales that were discussed earlier (and those that are discussed below) yield $D_f \simeq 1.2$, *inconsistent* with the fractal dimension of the RLCC aggregates. In other words, τ and D_f provide consistency checks on each other. Although there is no reason to believe that these aggregates can form by a percolation phenomenon, a process in which particles join randomly, we can also test whether percolation can be a plausible mechanism for the formation of the asphalt aggregates. For percolation in three dimensions, $\tau \simeq 2.18$. Thus, if in Eq. 13 we take this value of τ, since the slopes of all the scattering curves that were discussed earlier were about 1.8 at large length scales, we would obtain $D_f \simeq 2.2$, again inconsistent with the fractal dimension of percolation fractals $D_f \simeq 2.52$. Therefore, we believe that DLCC aggregation is the only sensible mechanism for the formation of the asphalt aggregates.

We must point out that the length scale (or the value of q) at which one has a crossover from the DLP aggregates to the DLCC ones depends on the composition of the oil, the type of solvent, and the temperature and pressure of the system. This length scale is not a universal property, and thus cannot be estimated from a knowledge of D_f and d_f alone.

We now investigate the effect of three important factors on the structure of these aggregates, namely, the temperature of the system, the type of solvent, and the aging of the asphalt-containing solution.

Effect of the temperature

In Figure 7 we present the logarithmic plots of $I(q)$ vs. q for two systems that contain 1% (by weight) asphalt, at 25°C and 43°C, reported by Sheu et al. (1992). The other characteristics of the solutions were the same as those discussed earlier. As this figure indicates, these experiments probed over more than one order of magnitude variations in the length scales, and the results are indicative of two important effects. First, since the concentration of the asphalt is very low, at the time of the measurements aggregate formation

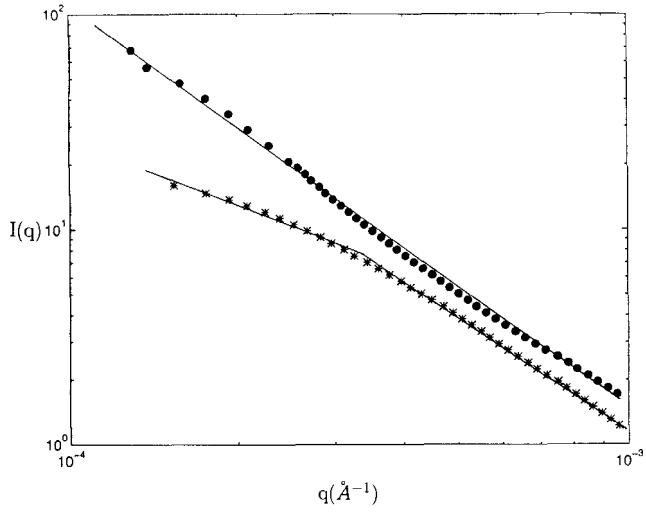

Figure 6. Logarithmic plot of scattering intensity $I(q)$ vs. the magnitude of scattering vector q for the data of Dwinggins (1978) for whole oil.

It shows the effect of the temperature; the results are for 25°C (top) and 80°C (bottom).

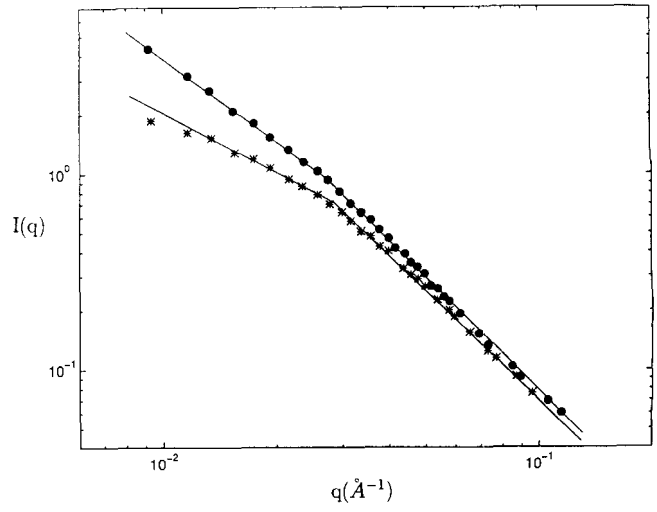

Figure 7. Logarithmic plot of scattering intensity $I(q)$ vs. the magnitude of scattering vector q for the data of Sheu et al. (1992).

It shows the effect of the temperature; the results are for 25°C (top) and 43°C (bottom).

had not been completed. Indeed, as the upper curve of Figure 7 (at 25°C) indicates, at large length scales (small q), the *effective* fractal dimension of the aggregates is only $D_f \simeq 1.42$, if we take $\tau = 2$, the value for the DLCC aggregates, and an even smaller D_f is we take $\tau = 3/2$, the value for the RLCC aggregates. At small length scales (large q), the slope is about 1.9 ± 0.1, indicating a d_f much lower than that of 3-D DLP aggregates, $d_f \simeq 2.5$. These results should be compared with the lower curves shown in Figure 3, which are for a solution that contains 5% asphalt. Second, increasing the temperature of the system has two consequences. One is that more resins are dissolved, and thus the electrical charge imbalance between the particles or small clusters is much lower. Thus, we expect to have aggregates with lower densities. The second, and the most important, consequence is that the rotational motion of the particles and clusters increases with rising temperature. It is known (Meakin, 1984) that, if during a DLCC aggregation process the clusters are allowed to rotate relatively fast, the fractal dimension of the DLCC aggregate *decreases*. For example, in 2-D simulation of DLCC aggregation, the fractal dimension decreases from $D_f \simeq 1.45$ for aggregates with no cluster rotational motion, to $D_f \simeq 1$ with very fast rotations (Meakin, 1984), with a similar phenomenon happening in 3D. Therefore, at high temperatures we expect to have asphaltene aggregates with lower fractal dimensions. This is clearly confirmed by the lower curves of Figure 7, which show the data at 43°C. At large length scales the slope of the line is 1.0 ± 0.1, which even with $\tau = 2$ yields $D_f \simeq 1 \pm 0.1$ for the aggregates, and with $\tau = 3/2$, one finds $D_f < 1$, an unphysical result. Even at small length scales, the clusters also have much smaller masses, and have organized themselves into clusters with a lower effective fractal dimension, since the slope of the line is only 1.8. This assertion is also supported by the results of Dwiggins (1978). He carried out SAXS experiments with a whole oil at two different temperatures. One was at 25°C, the results of which are shown as the upper curves in Figure 6, and were already described. The second scattering experiments were at 80°C, the results of which are shown as the lower curves in Figure 6. In complete agreement with our assertion, and consistent with the data of Sheu et al. (1992) discussed earlier, at large length scales the aggregate has a fractal dimension $D_f \simeq 1$, while at small length scales the fractal dimension is $d_f \simeq 1.75 \pm 0.05$. A different set of SAXS data was reported by Storm et al. (1993) at 93°C. These authors used an oil residue with n-heptane as the solvent to form asphalt. The resulting asphalt was solved in an asphalt-free residue (synthetic residue), with which the scattering experiments were carried out. The results (Figure 8) indicate that, over one order of magnitude variations in the length scales, a power-law scattering is observed. This figure also indicates that between an upper and a lower cutoff length scale, the aggregates are fractal with a fractal dimension, $D_f \simeq 1.1 \pm 0.1$, again in agreement with the results previously discussed. Figure 8 also demonstrates nicely how a small-angle scattering experiment can provide estimates of the lower and upper length scales for the fractality of a system.

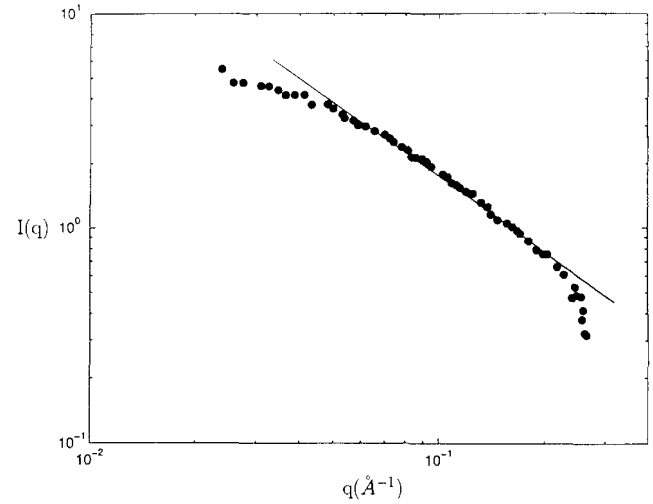

Figure 8. Logarithmic plot of scattering intensity $I(q)$ vs. the magnitude of scattering vector q for the data of Storm et al. (1993)

The results are for 93°C.

Aging effects

If the asphalt-containing solution is not aged for a long enough time, then one still obtains fractal aggregates, except that the formation of the aggregates is not complete, and thus the fractal dimensions of the aggregates represent *effective values* that may be *smaller* than their long-time values. For example, if the asphalt-containing solution that results in the lower curves of Figure 3 is not aged for 11 days, and the scattering experiment is carried out immediately after mixing of the asphalt-containing solution with toluene, one obtains the results that are shown as the upper curves in Figure 3. In this case, at large length scales the slope is about 1.66, which together with $\tau = 2$ yields $D_f \simeq 1.66$, smaller than that of 3-D aggregates, $D_f \simeq 1.8$ (see earlier), whereas at small length scales we have $d_f \simeq 1.94$, smaller than that of 3-D DLP aggregates, $d_f \simeq 2.5$. The reason for these values may be that the solution has not yet been aged for a long enough time, and thus aggregate formation has not been completed. Figure 9 also shows the effect of aging on the resulting aggregates. All the characteristics of the system are similar to those shown in Figure 3, except that the concentration of the asphalt particles in the solution is only 1%. The results indicate power-law scattering over one order of magnitude variations in the length scales. The upper curve in Figure 9 corresponds to the scattering results immediately after dispersion of the asphalt-containing solution in toluene, and indicates the existence of fractal aggregates with $D_f \simeq 1.14 \pm 0.07$. The lower curve is for a scattering experiment 11 days after the mixing and yields a fractal dimension $D_f \simeq 1.94 \pm 0.13$, consistent with $D_f \simeq 1.8$ for 3-D DLCC aggregates. Note that, as we discussed before, when the concentration of the solid particles is low, only one type of fractal aggregates is formed, and Figure 9 confirms this again.

Effect of the solvent

Most of the preceding results were obtained with n-heptane as the solvent. The only exception was the case with n-decane. All the results were also consistent with each other. We now discuss the scattering results with a completely different solvent, and then *speculate* on the possible effect of

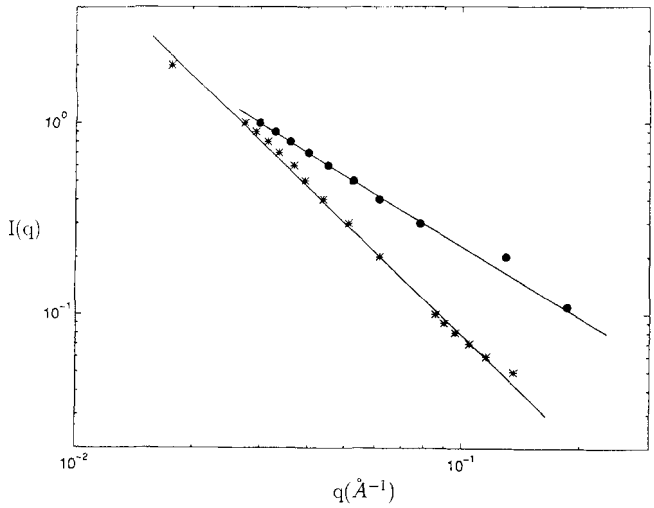

Figure 9. Logarithmic plot of scattering intensity $I(q)$ vs. the magnitude of scattering vector q for the data of Sheu et al. (1992) at 25°C.

It shows the effect of aging of the sample. The results are for immediately after mixing of the asphalt with toluene (top), and 11 days after the mixing (bottom). The concentration of the asphalt in the solution is 1%.

the solvent on the structure of the asphalt aggregates. Figure 10 presents the logarithmic plot of a SAXS experiment reported by Dwiggins (1978). In this experiment, *n*-propanol was used as the solvent at room temperature. The solution that was used for the scattering experiment contained about 50% (by weight) crude oil. Figure 10 indicates that there is only one type of fractal aggregate in the solution. The slope of the line is about 2.7 ± 0.06, inconsistent with a DLCC structure for which $D_f(3-\tau) \simeq 1.8$ (see Eq. 13), and with a RLCC structure for which $D_f(3-\tau) \simeq 3.07$. Thus, what is the interpretation of this result? At this point we can only speculate, since we do not have enough information about the experiments, nor do we have any data for any other type of

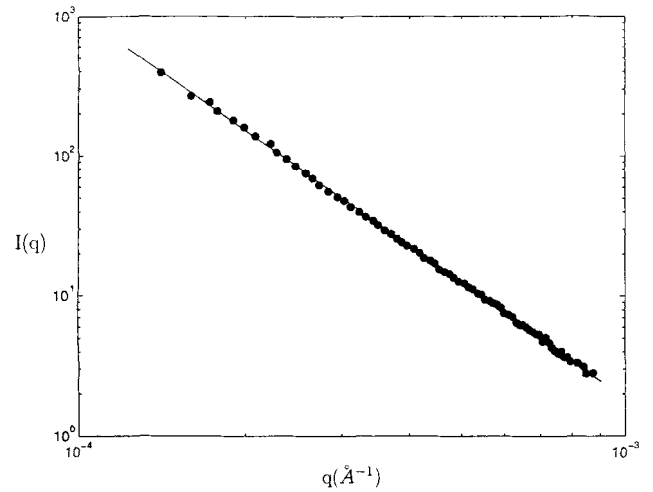

Figure 10. Logarithmic plot of scattering intensity $I(q)$ vs. the magnitude of scattering vector q for the data of Dwinggins (1978), with propanol as the solvent.

solvent other than what we are discussing here. Moreover, the range of the length scales probed in these experiments is not broad enough to draw any definitive conclusion from the results. However, we note that Jullien and Hasmy (1995) have argued that, if in the DLCC aggregation model the initial concentration of the particles is larger than a critical value, then instead of the usual DLCC aggregate one may obtain a gel network with a fractal structure. The fractal dimension of the gel network (at the gel point) is about $D_f \simeq 2.52$ (for a review of gelatin models and their fractal structures, see Sahimi, 1992, 1994). If we assume that the solution essentially contains one large aggregate, so that, instead of Eq. 13, Eq. 11 is applicable, then one has an aggregate with a fractal dimension $D_f \simeq 2.7$, only 7% larger than that of gels. Since the concentration of the crude oil in the propanol was very high, it is possible that the concentration of the asphalt particles was above the critical value for gel formation, and therefore a gel network was formed. One may also speculate that, the presence of propanol in the solution created hydrogen bonds that bridged the small clusters, which otherwise would not have been attached to each other. As a result, a much denser fractal aggregate with higher D_f was formed.

Scaling Analysis of the Precipitation Data

We now consider the problem from a completely different angle, namely, the precipitation of the asphalt aggregates, and show that the *amount* of the precipitated aggregates also provides insight into their structure, and that the results are in agreement with the small-angle scattering data. To measure the amount of the precipitated aggregates we used a crude oil that we filtered to remove its solid contents, such as sand. We then diluted the oil by a solvent, which was an *n*-alkane with a carbon number ranging from 5 to 10. Several different dilution ratios R, measured in terms of the cm^3 of the agent/g of the oil, were used. The diluted oil was then agitated in a tube, which caused the formation and precipitation of the aggregates. After one day the solid content of the oil, that is, the precipitated aggregates, was measured. During the entire experiment the temperature was kept at about 25°C. Complete details of the experiments are given in Part I.

Figure 11 shows our experimental results for the weight percent of the precipitated asphalt W, in weight of the asphalt/g of the crude oil, for five different solvents (*n*-alkanes) and various solvent to crude ratios R. (Some of these data were reported in Part I, and are presented here only for the following discussion.) These results are strongly suggestive of the possibility that a scaling equation may be developed for predicting them, since all the curves start at about the same point, and at large values of R they become more or less parallel. As a result, it may be possible to collapse the data onto a single scaling curve. This is in fact typical of aggregation processes. For example, one can calculate the cluster-size distribution $n_s(t)$, discussed earlier, as a function of either the cluster size s at a fixed time t, or as a function of t at a fixed s. This has been studied in detail by Meakin et al. (1985). However, Eq. 3 also tells us that we can collapse all the cluster-size distributions onto a single curve, if we plot $s^{\tau}n_s(t)$ vs. $s/\langle s\rangle$ (with $\langle s\rangle \sim t^{w}$), since the scaling function $f(s/\langle s\rangle)$ is *universal* and does not depend on the details of the system. Figure 12 shows the results of this collapse, which confirms Eq. 3 with $\tau = 2$.

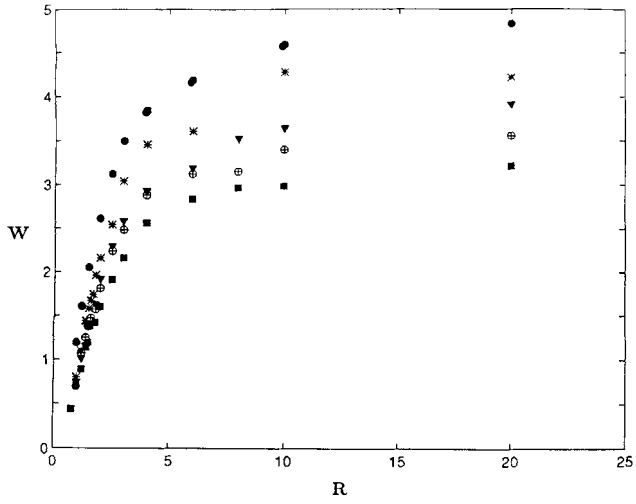

Figure 11. Experimental precipitation data for weight percent *W* of asphalt aggregates, as a function of the solvent to crude ratio *R*.

The results are, from top to bottom, for $n-C_5$, $n-C_6$, $n-C_7$, $n-C_8$, and $n-C_{10}$ as the solvent.

Since the small-angle scattering data previously analyzed already suggest that asphalts and asphaltenes are fractal aggregates with well-defined scaling properties, the data collapse should be possible, and this is indeed the case. The variables in Figure 11 are R, W, and M, the molecular weight of the solvent. We find that, if we let $X = R/M^z$ and $Y = WR^{z'}$, then all the experimental data shown in Figure 11 can be collapsed onto a single curve with

$$z = \frac{1}{4}, \qquad z' = 2, \tag{14}$$

where the estimated error bars are about $\pm 5\%$. The resulting data collapse is shown in Figure 13. Note that, we could not find any other values for z and z' that could collapse the precipitation data onto a single curve with the same accuracy, nor could we find any other combinations of the three variables that collapse the data onto a single curve. Thus, these combinations of the variables and the values of z and z' appear to be unique.

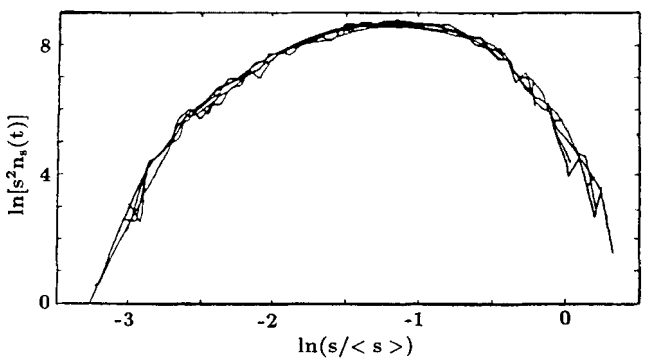

Figure 12. Collapse of cluster-size distribution $n_s(t)$ of DLCC aggregates onto a single curve.

Adopted from Meakin et al., 1985.

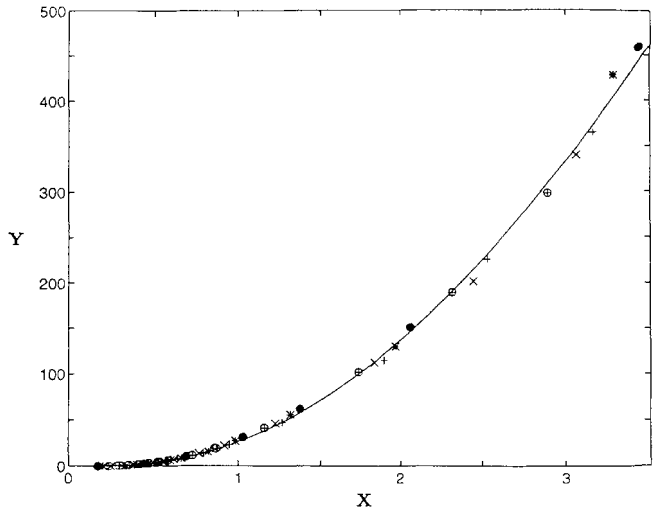

Figure 13. Collapse of experimental precipitation data of Figure 11, where $X = R/M^z$ and $Y = WR^{z'}$, with $z = 1/4$ and $z' = 2$.

In Part I the exponents z and z' were given without providing any theoretical explanation for their values, nor could we explain why the precipitation data can be collapsed onto a single curve. However, based on the dynamic cluster-size distribution for the DLCC aggregates, we can now provide a theoretical explanation for both of these. If we combine Eqs. 3 and 5, and take $\tau = 2$, the value for the DLCC aggregates, we obtain

$$s^2 n_s(t) = f(s/t^w), \tag{15}$$

which implies that the universal scaling function $f(x)$ can be expressed only in terms of $s^2 n_s(t)$. On the other hand, if the scaling function shown in Figure 13 is written as $Y = h(X)$, where $h(X)$ is the curve representing the collapsed data, then the data collapse shown in Figure 13 implies that

$$R^2 W = h(R/M^z), \tag{16}$$

which is completely similar to Eq. 15, offers a plausible explanation for the collapse of the precipitation data onto a single curve and the value $z' = 2$, and indicates that, as we argued earlier, the clusters have the structure of the DLCC aggregates. Of course, the scaling functions $f(x)$ and $h(x)$ are not the same. Comparing Eqs. 15 and 16, one may infer that the *roles* of s and $n_s(t)$ in the dynamic cluster-size distribution are played by R and $W(t)$, respectively. It is not unreasonable to infer that the size of the asphalt aggregates may be proportional to the ratio R, and indeed as Figure 11 indicates with increasing R the amount of precipitation, and thus the size of the aggregates, do increase. As a rough estimate, $W(t)$ is also proportional to $n_s(t)$, the number of clusters or aggregates of size s at time t for *all* $s \geq s_{\min}$. Here $s_{\min}$ is the minimum cluster size for precipitation, since only when a cluster is large enough, can it precipitate; otherwise it will remain suspended in the solution. We expect to have $s_{\min} \sim \alpha\langle s\rangle$, where $\alpha > 1$. With these analogies, it becomes clear why the data collapse shown in Figure 13 is possible. How-

ever, one has to be careful with such analogies, since although we expect $W(t)$ to be related to $n_s(t)$, the relation between them is more complex than a simple proportionality. In fact, we expect the weight percent of precipitated asphalt $W(t)$ to be related to $n_s(t)$ by the following equation

$$W(t) \sim \int_{\alpha\langle s\rangle}^{\infty} s n_s(t)\, ds, \tag{17}$$

that is, $W(t)$ is simply proportional to the sum of the sizes of all the clusters that are larger than $s_{\min} \sim \alpha\langle s\rangle$. The analogy between Eqs. 15 and 16 also implies that the *role* of the mean cluster size $\langle s\rangle \sim t^w$ in the dynamic cluster-size distribution, Eq. 15, is played by M^z in the scaling equation for the precipitation data, Eq. 16. That is, the mean size of the asphalt aggregates is proportional to the molecular weight M of the solvent, raised to some power z. Since Eq. 5 tells that the exponent w depends on ζ, the exponent that relates the diffusivity of an aggregate to its molecular weight, $\mathfrak{D} \sim M^{\zeta}$, we also conclude that the exponent z, the analog of w, may also be nonuniversal and presumably depend on the type of solvent and/or asphalt-containing oil, whereas the exponent $z' = 2$ is universal and does not depend on the solvent or the oil type. This universality is the result of mass conservation in the system, which also results in Eq. 3 with $\tau = 2$.

We now make another quantitative connection between the scattering results and the precipitation data, and show that the latter also indicate that $D_f \simeq 1.8$ and $d_f \simeq 2.5$. To do this, we assume that the distribution of the asphalt aggregates does obey Eq. 3; we also derive an expression for the mass of the aggregates in the solution and show that the results are consistent with the precipitation data only if $\tau = 2$, $d_f \simeq 2.5$, and $D_f \simeq 1.8$. For a cluster of size s the radius is $R_p(s) \sim s^{1/D_f}$, and its volume is $v \sim s^{3/D_f}$. Thus the volume of the clusters or aggregates in the solution is

$$V \sim \int_0^{\alpha\langle s\rangle} v n_s(t)\, ds, \tag{18}$$

which, when combined with Eq. 3, yields

$$V \sim \int_0^{\alpha\langle s\rangle} s^{3/D_f} s^{-\tau} f(s/\langle s\rangle)\, ds$$

$$= \langle s\rangle^{3/D_f - \tau + 1} \int_0^{\alpha} x^{3/D_f - \tau} f(x)\, dx \sim \langle s\rangle^{3/D_f - \tau + 1}. \tag{19}$$

Note that the limits of the integrals in Eqs. 17–19 are different. Equation 17 is for the large aggregates that have precipitated (whose minimum size is about $\alpha\langle s\rangle$), while Eqs. 18 and 19 are for those that have remained in the solution. If v_t is the volume of a *typical* cluster or aggregate in the solution, then Eq. 19 is written as $V \sim v_t^{[3+D_f(1-\tau)]/3}$. In a solution that contains one or a few large aggregates with a fractal dimension D_f and a large number of small aggregates with a fractal dimension d_f, the typical or average aggregate size is dominated by those of the small aggregates. That is, the mean size of the aggregates *remaining in the solution* is dominated by the small aggregates (since if they had been large enough, they would have precipitated). Therefore, we can write $v_t \sim l^{d_f}$, where l is the radius of the typical aggregates. Combining this equation with Eq. 19, and noticing that the mass m of the aggregates in the solution is $m = \rho V$, where ρ is the aggregate density, we obtain

$$m \sim \rho l^{d_f[3+D_f(1-\tau)]/3}. \tag{20}$$

Equation 20 tells us that a logarithmic plot of m vs. l should yield a straight line with a slope $p = d_f[3 + D_f(1-\tau)]/3$. If our interpretation of the small-angle scattering results is correct, then $\tau = 2$, $d_f \simeq 2.5$, and $D_f \simeq 1.8$, which means that the slope of the line should be $p \simeq 1.0$. The only quantity to be specified is l, which is very difficult to measure directly. Since asphalt and asphaltene aggregates are fractal with complex shapes, one can estimate l only if the fractal aggregate is approximated by a simple shape. For example, Herzog et al. (1988) and Acevedo et al. (1994) suggested that one may represent asphalts roughly as relatively thin discs, whose thickness was estimated to be in the range 3.6–8.0 Å, while the density of asphalt aggregates is typically about 1.1–1.3 g/cm^3. Thus, if, as a rough estimate, we assume l to be the radius of the discs, given the weight and density of the asphalts in the solution and the thickness of the discs, which we took it to be 5.8 Å, l can be estimated. We found that for a fixed dilution ratio R a plot of $\ln m$ vs. $\ln l$ does reproduce straight lines whose slopes vary between 0.9 and 1.13, with an average of about 1.03, in agreement with the theoretical prediction $p \simeq 1.0$.

Our recent measurements of the MW distributions of asphalts and asphaltenes with various solvents and dilution ratios R (Dabir et al., 1996) suggest that heavier solvents with larger molecular diameters also generate larger aggregates, resulting in broader MW distributions. As pointed out earlier, the analogy between Eqs. 15 and 16 also implies that the mean aggregate size is directly related to the molecular weight of the solvent. Thus, we may also assume l to be proportional to some characteristic length scale of the solvent molecules, such as their effective molecular diameter, or, since we used n-alkanes as the solvent, their linear dimension. However, for n-alkanes the effective molecular diameter is directly proportional to their linear dimension, and therefore any one of them can be used. For the n-alkanes the values of l, taken as the effective molecular diameter, are available in standard handbooks. Figure 14 shows the plots of $\ln m$ (calculated from Figure 11) vs. $\ln l$ for various n-alkanes and values of the dilution ratio R, where on each line R is constant. As can be seen, all the lines for the various n-alkanes and Rs are parallel to one another as they should be, since their slope depends only on the universal quantities τ, d_f, and D_f. Moreover, we find that $p \simeq 1.05$, in excellent agreement with both the theoretical expectation $p \simeq 1.0$ and $p \simeq 1.03$ obtained by assuming that the aggregates can be represented as thin discs. Therefore, not only are the precipitation data consistent with a dynamic cluster-size distribution for fractal diffusion-limited aggregates, they also indicate that the fractal dimensions of the aggregates are the same as those that we infer from the scattering data. Note that, only if we take $\tau = 2$ and have two types of aggregates in the solution with two different fractal dimensions d_f and D_f, do the predictions of Eq. 20 agree with the data, thus supporting our interpretation of the scat-

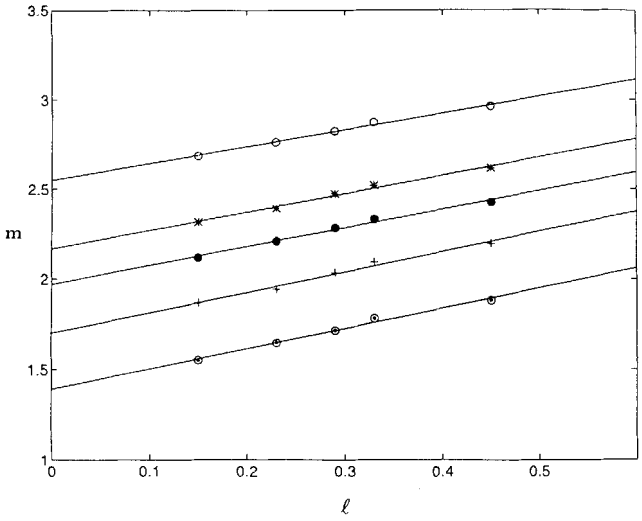

Figure 14. Logarithmic plot of weight *m* of asphalt aggregates remaining in the solution vs. molecular diameter *l*.

Symbols are the same as in Figure 11, and on each line the symbols show the data at a fixed ratio R. The results are, from top to bottom, for $R = 2, 4, 6, 10$, and 20.

tering data. All other plausible values of τ, d_f, and D_f yield slopes that do agree with the experimental value, $p \simeq 1.05$.

We should point out that an equation similar to Eq. 20 with $\tau = 2$ was given previously by Crickmore and Hruska (1989) (CH) using a completely different derivation. However, in their derivation they made a *wrong* assumption, but still obtained the same result as ours! They assumed that d_f (whose origin they did not specify) is the fractal dimension of the *largest* asphalt aggregate (which is, in fact, D_f), whereas as our discussion here makes clear, d_f is the fractal dimension of the *typical* or average-size aggregates, which are dominated by the small DLP clusters. Janardhan and Mansoori (1993) attempted to derive the equation given by CH, made the same error they did, and applied the equation erroneously to some precipitation data at *the onset of the precipitation*. At this point, the dilution ratio R_c is different for various solvents, and therefore there is no way of obtaining the type of straight lines shown in Figure 14, since on each line the dilution ratio is constant for all the solvents. It is not clear to us how they obtained the results that they present in their article.

Summarizing the results of the last two sections, almost all the different sets of small-angle scattering data as well as the precipitation results, *for completely different oils* and aggregate sizes ranging from 50 Å to over 7,000 Å, yield the *same result*: The largest asphalt particles are DLCC aggregates with a *universal* fractal dimension $D_f \simeq 1.8$ (independent of the type of the oil), whereas the small asphalt particles are DLP aggregates with a *universal* $d_f \simeq 2.5$. As discussed earlier, high temperatures can generate low-density aggregates with lower *effective* fractal dimensions, because they increase rotational motion of the diffusing clusters in the solution. Moreover, if the concentration of the solid particles in the oil is low, eventually only the DLCC aggregates will form. Thus, we can identify both the fractal dimension of these aggregates and the mechanisms of their formation. These results are also supported by the recent experiments of Toulhoat et al. (1994). Using atomic force microscopy, they obtained beautiful pictures of asphalt aggregates that are completely similar to those shown in Figure 1, and thus providing strong support for our results.

We should mention that, in the past there has been some speculation about the possibility of asphalts and asphaltenes having a fractal structure (Park and Mansoori, 1988; Crickmore and Hruska, 1989; Lin et al., 1991; Kuzeev et al., 1991; Mukhametzyanov and Kuzeev, 1991; Raghunathan, 1991; Liu et al., 1995). However, aside from Liu et al. (1995), none of these authors specified what kind of a fractal structure the asphalt and asphaltene aggregates may possess, or proposed any mechanism for their formation. In the absence of any mechanism for the formation of a fractal structure with a given dimension, one can, in principle, have an infinite number of ways by which the fractal structure may form. In fact, Park and Mansoori (1988), Crickmore and Hruska (1989), and Lin et al. (1991) all stated that, if the asphalt and asphaltene aggregates are fractal, *their fractal structures and fractal dimensions cannot be specified*, and Raghunathan (1991) speculated that the fractal structure of these aggregates is similar to that of *linear polymers* whose fractal dimension is $D_f \simeq 5/3$. Liu et al. (1995) proposed that if the concentration of the asphalt aggregates in the solution is high or low, then one has nonfractal aggregates, whereas in the intermediate regime one has the RLCC aggregates. However, their own data suggest that $\tau \simeq 1.8 \pm 0.2$, much closer to $\tau = 2$ for the DLCC aggregates than to $\tau = 3/2$ for the RLCC aggregates. While we agree with them regarding nonfractality (and compactness) of the aggregates if their concentration in the solution is very high (see earlier), we disagree with them about the low concentration regime. We must also emphasize that a fractal dimension $D_f \simeq 1.8$ does *not* imply that the aggregates are nearly two dimensional. It only means that the number of the elementary solid particles in the aggregates is so low that their fractal dimension is smaller than two. But, such aggregates still have a 3-D structure, that is, they cannot be placed on a plane, or even on a few planes.

Finally, we point out that there is no shortage of broad conceptual models of asphalts and asphaltenes structure in the literature. Over the years, many models have been proposed, beginning perhaps with the work of Dickie and coworkers (1967, 1969), in which an analogy to polymers was proposed. Many other conceptual models have been proposed (see, for example, Yen, 1974; Ignasiak et al., 1977a,b; Speight and Moschopedis, 1980; Sakai et al., 1983; Boduszynski, 1987, 1988; Sane et al., 1988; Nortz et al., 1990; Strausz et al., 1992). In particular, an interesting model has been proposed by Klein and coworkers (Savage and Klein, 1989; Truath et al., 1994), in which the experimental knowledge about the chemical structure of asphaltenes has been used for developing a model that combines experimental data and an iterative stochastic method for generating a model of asphaltenes. However, it is not clear to us that their model can yield molecular structures similar to what we propose here.

Implications of the Results

The discovery that asphalt particles are fractal aggregates implies that the vast knowledge already available for such ag-

gregates can be used immediately to study in detail the structure of the asphalts and the kinetics of their formation. Here we discuss three important consequences of our results, which are modeling aggregation and flocculation of the asphalt particles, their mechanical stability, and their molecular-weight distribution.

Modeling Kinetics of Aggregation of the Asphalt Particles

The kinetics of aggregation of many colloidal particles can be described in terms of the Smoluchowski equation

$$\frac{dn_k}{dt} = \frac{1}{2}\sum_{i+j=k}^{k-1} K(i,j)n_i n_j - n_k \sum_{i=1}^{\infty} K(k,i)n_i, \quad (21)$$

where n_i is the number of clusters or aggregates of size i, and $K(i,j)$ is a collision matrix or kernel, which is a function of both the collision of the clusters and the aggregation processes. The first term of the righthand side of Eq. 21 represents the formation of clusters of size k from the two smaller clusters of sizes and $j = k - i$, while the second term represents the loss of the clusters of size k by reaction with other clusters to form larger clusters. This equation is based on the assumption that the collision between the clusters or aggregates, or the asphalt particles in our problem, is random and binary. The assumption of randomness is valid if the fluctuations in the density of the particles is small. Such an assumption makes the equation a mean-field approximation, and mean-field approximations are valid only above a certain spatial dimension d which, in our case, is $d = 2$. Thus, the Smoluchowski equation is valid for describing aggregation of the asphalt and asphaltene particles.

The most important parameter of the Smoluchowski equation is the kernel $K(i,j)$ and its functional form. For many processes to which the Smoluchowski equation may be applicable, it is *not* clear *a priori* what functional form one should use for the kernel. Ziff et al. (1985) carried out extensive computer simulations of DLCC aggregation in three dimensions, and showed that

$$K(i,j) \sim (i^{\zeta} + j^{\zeta})(i^{1/D_f} + j^{1/D_f}), \quad (22)$$

where ζ is the exponent that relates the diffusivity of the cluster to its molecular weight, $\mathfrak{D} \sim M^{\zeta}$, defined earlier. Thus, Eq. 22 can be used immediately to study the kinetics of asphalt and asphaltene aggregation by the Smoluchowski equation.

Mechanical Stability of the Asphalt Aggregates and an Upper Bound to Their Molecular Weight

One of the most interesting aspects of fractal aggregates is that their density can be much smaller than that of their constituent particles, and it decreases as their size increases. But, at the same time, fractal aggregates can preserve their mechanical stability and support deformation. Therefore, it is sensible to ask how large fractal aggregates can become before losing their mechanical stability, which would force them to recognize themselves into a more stable structure.

Consider first a nonfractal object. Suppose that the system is at a temperature T, and that the material at a distance r from the origin is displaced by an amount u, which produces a strain $\epsilon \sim u/r$. Suppose also that the shear modulus of the system is μ. Thus, the displacement of the system costs an elastic energy per unit volume of the system, which is about $\mu\epsilon^2$. With thermal fluctuations in the system we must have $k_B T \sim \mu\epsilon^2 r^d$, where r^d is the volume of the system, and k_B is the Boltzmann constant, and thus $\epsilon^2 \sim r^{-d}$.

Consider now fractal aggregates. We must distinguish between fractal aggregates with many closed loops of particles at any length scale, such as gel networks at the gelation point, and those that contain small and insignificant (in a macroscopic sense) loops, such as the DLCC and DLP aggregates (see Figures 1 and 2). In loopless fractals there is essentially only one path connecting two widely separated points in the system, which is called the *minimum path*. Suppose that we fix one of the points at the origin, and displace the other one by an amount u. Since the fractal is loopless, displacement of the particle strains only the essentially one-dimensional path between the displaced particle and the one at the origin (the same argument *cannot* be used for fractals with large loops, since there are more than one path between the two points). Suppose that the number of the elementary particles in the path is n_p, and that their effective size is a. If r is large, then

$$n_p \sim r^{D_{\min}}, \quad (23)$$

where $D_{\min}$ is called the fractal dimension of the minimum path. In general, $D_{\min} > 1$, but for the DLP aggregates $D_{\min} \simeq 1$, while for the DLCC aggregates in 3-D $D_{\min} \simeq 1.25$. Kantor and Witten (1984) showed that

$$\epsilon^2 \sim \frac{k_B T}{\mu b^d n_a}\left(\frac{r}{a}\right)^{D_{\min}}. \quad (24)$$

In this equation, b^d is the volume of the atoms that constitute the particles, and n_a is the number of atoms in a particle. Thus, the average strain *increases* with the length scale r, $\epsilon \sim r^{D_{\min}}$, in contrast with nonfractal objects for which $\epsilon \sim r^{-d}$. If r and n_p are larger than some critical values r_c and n_{pc}, ϵ becomes of the order of unity. If an aggregate is larger than this critical size n_{pc}, it becomes flexible and is free to respond to internal forces in the same way as polymers do. If the forces are attractive, then the aggregate attains a *collapsed* state. For colloidal particles, such as asphalt and asphaltene aggregates, n_a is typically about 10^3, μb^d is about 10 eV, while $k_B T$ is about 1/40 eV at room temperature. Thus, the maximum value that n_p can take is about 10^4, before thermal fluctuations distort the aggregate and force it to reorganize itself into another more stable structure. Thus, fractal structures, such as the asphalt and asphaltene aggregates, *cannot* become too large. This restriction places an upper bound on the average molecular weight that an asphalt or asphaltene aggregate can attain, which is about 6,000–10,000. In the literature, one finds estimates of the average molecular weight of the asphalt or asphaltene aggregates that are as large as 10^5–10^6. In the light of what we discuss here, such claims are wrong.

Molecular-Weight Distribution of the Asphalt Aggregates

The MW distribution is, in general, a time-dependent quantity that evolves as the aggregation of the asphalt and asphaltene particles takes place. Since the asphalt and asphaltene aggregates are of the DLP and DLCC type, a measure of their MW distribution is provided by their cluster-size distribution, Eq. 3. Because the Smoluchowski equation can be used to determine the cluster-size distribution, one can, in principle, also use the same equation to study the time-evolution of the MW distribution. However, what we are interested in here is the MW distribution of the aggregates after a long time. Over the years, many authors have studied this problem (Dickie and Yen, 1967; Moschopedis and Speight, 1976; Moschopedis et al., 1976; Boduszynski et al., 1977; Ignasiak et al., 1977a,b; Speight and Moschopedis, 1977; Schwager and Yen, 1978; Snape and Bartle, 1984; Speight et al., 1985; Boduszynski, 1987, 1988; Acevedo et al., 1992; Strausz et al., 1992; Taylor, 1992; Trauth et al., 1994). Aside from Trauth et al. (1994), these authors mainly measured the average MW of asphalts and asphaltenes from various oils, and provided some statistics of their measurements, but none proposed an analytical formula for the MW distribution, and in fact they did not even give the full MW distribution itself. Trauth et al. (1994) used a Monte Carlo method to determine the MW distribution, based on their own model described earlier.

Botet and Jullien (1984) studied the cluster-size distribution during DLCC aggregation processes. They derived an analytical formula for the *most probable* cluster-size distribution, and also determined numerically the *average* cluster-size distribution (since it cannot be calculated analytically in closed form), where the averaging was taken with respect to the process time. Suppose that at the beginning of the aggregation process there are N particles, and that there are N_c clusters or aggregates in the system. Botet and Jullien (1984) showed that the most probable cluster-size distribution is given by

$$\frac{Nn_s}{N_c^2} \sim f_\omega(N_c s/N), \tag{25}$$

where ω is defined by Eq. 2. Equation 25 tells us that $f_\omega(x)$ can be considered as a rescaled or reduced most probable cluster-size distribution. Subject to certain assumptions, Botet and Jullien (1984) also derived the following equation for $f_\omega(x)$

$$f_\omega(x) = \frac{(1-2\omega)^{1-2\omega}}{\Gamma(1-2\omega)} x^{-2\omega} \exp[-(1-2\omega)x]. \tag{26}$$

This equation can have a maximum only if $\omega < 0$. Botet and Jullien compared Eq. 26 with their numerical simulations and showed that, except around the maximum of the distribution where Eq. 26 does not always estimate the magnitude of the maximum very accurately, it provides a very accurate description of the cluster-size distribution.

We now convert Eq. 26 to a MW distribution for the asphalt and asphaltene aggregates by assuming that the molecular weight of an aggregate is proportional to its size. Experimental measurements also show that there is usually a minimum molecular weight M_m at which the MW distribution is cutoff. Therefore, Eq. 26 implies the following equation for the MW distribution for asphalts and asphaltenes:

$$f_\omega(M) = c_1(M - M_m)^{-2\omega} \exp[-c_2(M - M_m)], \quad M \geq M_m, \tag{27}$$

where c_1 and c_2 are constants. The normalization condition, $\int_0^\infty f_\omega(M)\,dM = 1$, gives one relation between c_1 and c_2, so that Eq. 27 has one free parameter to adjust. In Eq. 27 we can treat ω as an adjustable parameter, but in what follows we provide evidence that ω may in fact be a *universal* exponent, and thus its value can be fixed.

We used Eq. 27 to fit the experimental data presented by Park and Mansoori (1988). The data are for the asphalt MW distributions in Brookhaven oil, obtained with three different n-alkanes. For all three cases we obtained

$$\omega \simeq -0.14 \pm 0.03, \tag{28}$$

indicating that, at least for n-alkanes, the value of ω is universal. That ω is found to be negative is expected, since, as mentioned previously, Eqs. 26 and 27 can have a maximum only if ω is negative. Figure 15 compares our fits with the data. As can be seen, except around the maximum of the distributions, the agreement between the predictions and the data is excellent. The slight disagreement between the predictions and the data around the maximum is expected, since, as discussed earlier, Botet and Jullien (1984) have already shown that Eq. 26 may underestimate the magnitude of the maximum of the cluster-size distribution, consistent with Figure 15. The small value of ω also has two implications for the structure of the asphalt and asphaltene aggregates. First, it implies that the active surface area of the aggregates that actually participates in the process is very small. This is partly

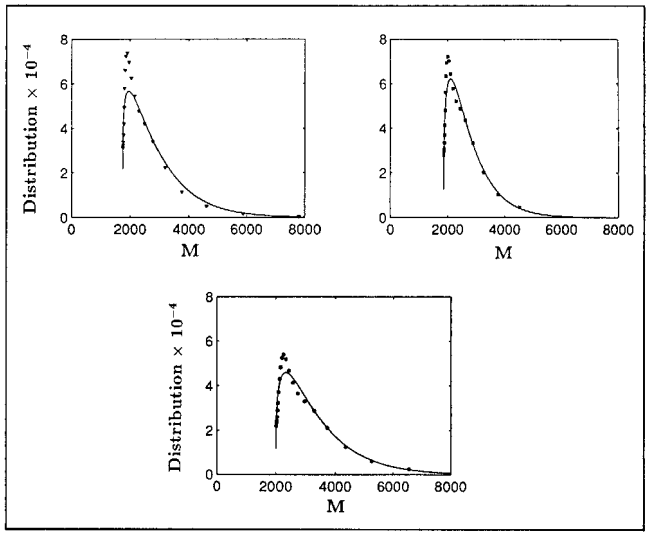

Figure 15. Predictions of Eq. 27 (curves) vs. experimental data of Park and Mansoori (1988) for molecular weight *M* of asphalt aggregates.

The results are for $n - C_5$ (top left), $n - C_6$ (top right), and $n - C_7$ (bottom) as the solvent.

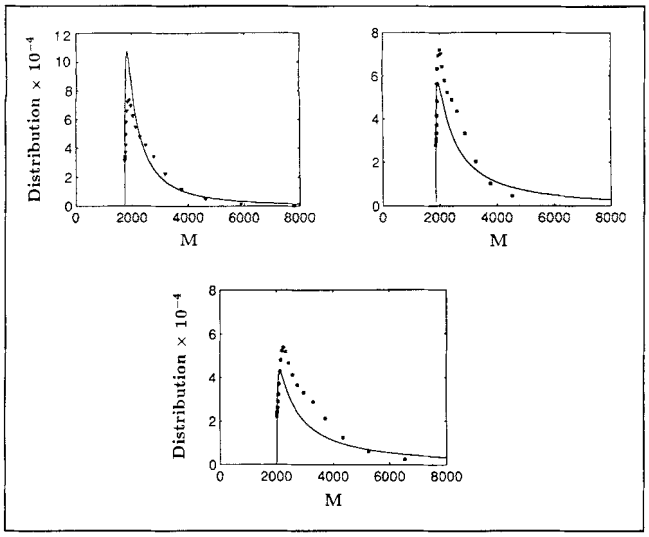

Figure 16. Predictions of Eq. 29 (curves) vs. experimental data of Park and Mansoori (1988) for molecular weight *M* of asphalt aggregates.

Symbols are the same as those in Figure 15.

due to the rough and irregular, and possibly fractal, nature of the aggregates' surface, and partly due to the fact that no solvent can dissolve all the resins that cover the surface of the solid particles that are suspended in the oil, which are the building blocks of the aggregates. Second, $\omega < 0$ implies that as the size of the aggregates increases, their active surface area *decreases*, since an increase in the aggregate size also increases the roughness of its surface.

As mentioned earlier, some authors have suggested an analogy between the structure of the asphalt and asphaltene aggregates, and polymers. In the polymer literature, use of a log-normal distribution for representing the MW distribution of polymers is popular. Therefore, we thought it may be useful to also use a log-normal distribution for predicting the preceding data, and compare the results with the predictions of Eq. 27. Hence we used

$$f(M) = \frac{1}{\sqrt{2\pi}\,\sigma(M - M_m)} \exp\Big\{ -[\ln(M - M_m) - \ln\langle M\rangle]^2 / 2\sigma^2 \Big\}, \quad (29)$$

where $\langle M\rangle$ and σ are the mean and standard deviation of the distribution, respectively, which we treated as adjustable parameters. The resulting fits of the data are shown in Figure 16, and it is clear that they do not agree with the data. Elsewhere (Dabir et al., 1996) we present new and extensive data for the MW distribution of asphalts and asphaltenes, and discuss their theoretical prediction using the ideas discussed here.

Summary and Conclusions

We have analyzed extensive small-angle scattering and precipitation data in order to delineate the structure of asphalt and asphaltene aggregates. Almost all the data, with various oils and solvents, provide compelling evidence that the asphalt and asphaltene aggregates are fractal objects with well-defined structures and fractal dimensions. Moreover, the *mechanisms* of their formation also become clear: At short length scales, the aggregates are formed by a diffusion-limited *particle* aggregation process, while at large length scales they are due to a diffusion-limited *cluster–cluster* aggregation process. We have also shown that the type of solvent and the temperature of the system both have a strong influence on the structure of the aggregates, and that the fractal structure of the aggregates places an upper bound on their size and average molecular weight. Finally, we have proposed a new molecular-weight distribution for the asphalt and asphaltene aggregates, which provides very good predictions for the experimental data.

Acknowledgments

This work was supported in part by the Department of Energy. We would like to thank Ali R. Mehrabi for his expert help in computing the molecular-weight distributions.

Literature Cited

Acevedo, S., G. Escobar, M. A. Ranaudo, and L. Gutiérrez, "Discotic Shape of Asphaltenes Obtained from g.p.c. Data," *Fuel*, **73**, 1807 (1994).

Acevedo, S., G. Escobar, L. Gutiérrez, and H. Rivas, "Isolation and Characterization of Natural Surfactants from Extra Heavy Crude Oils, Asphaltenes and Maltenes," *Fuel*, **71**, 619 (1992).

Ball, R. C., D. A. Weitz, T. A. Witten, and F. Leyvraz, "Universal Kinetics in Reaction-Limited Aggregation," *Phys. Rev. Lett.*, **58**, 274 (1987).

Baltus, R. E., and J. L. Anderson, "Asphaltene Characterization and Diffusion Measurements," *Chem. Eng. Sci.*, **38**, 1959 (1983).

Boduszynski, M. M., "Composition of Heavy Petroleums. 1. Molecular Weight, Hydrogen Deficiency, and Heteroatom Concentration as a Function of Atmospheric Equivalent Boiling Point up to 1400°F," *Energy & Fuels*, **1**, 2 (1987).

Boduszynski, M. M., "Composition of Heavy Petroleums. 2. Molecular Characterization," *Energy & Fuels*, **2**, 597 (1988).

Boduszynski, M. M., B. Raj Chadha, and T. Szkutta-Pochopien, "Investigations of Romashkino Asphaltic Bitumen. 3. Fractionation of Asphaltenes Using Ion-Exchange Chromatography," *Fuel*, **56**, 434 (1977).

Botet, R., and R. Jullien, "Size Distribution of Clusters in Irreversible Kinetic Aggregation," *J. Phys. A*, **17**, 2517 (1984).

Bouchaud, E., M. Delsanti, M. Adam, M. Daoud, and M. Durand, "Gelation and Percolation: Swelling Effect," *J. Phys.*, **47**, 1273 (1986).

Crickmore, P. J., and C. Hruska, "Fractal Geometry, the Korčak Law and Asphaltene Precipitation," *Fuel*, **68**, 1488 (1989).

Dabir, B., M. Nematy, A. R. Mehrabi, H. Rassamdana, and M. Sahimi, "Asphalt Flocculation and Deposition: III. The Molecular Weight Distribution," *Fuel*, **75** (1996).

Dickie, J. P., M. N. Haller, and T. F. Yen, "Electron Microscopic Investigations on the Nature of Petroleum Asphaltics," *J. Colloid Interf. Sci.*, **29**, 475 (1969).

Dickie, J. P., and T. F. Yen, "Macrostructures of the Asphaltic Fractions by Various Instrumental Methods," *Anal. Chem.*, **39**, 1847 (1967).

Dwiggings, C. W., "Study of the Colloidal Nature of Petroleum with an Automated Bonse-Hart X-Ray Small-Angle Scattering Unit," *J. Appl. Cryst.*, **11**, 615 (1978).

Herzog, P., D. Tchoubar, and D. Espinat, "Macrostructure of Asphaltene Dispersions by Small-Angle X-Ray Scattering," *Fuel*, **67**, 245 (1988).

Ignasiak, T., A. V. Kemp-Jones, and O. P. Strausz, "The Molecular Structure of Athabasca Asphaltene. Cleavage of the Carbon-Sulfur Bonds by Radical Ion Electron Transfer Reactions," *J. Org. Chem.*, **42**, 312 (1977a).

Ignasiak, T., O. P. Strausz, and D. S. Montgomery, "Oxygen Distribution and Hydrogen Bonding in Athabasca Asphaltene," *Fuel*, **56**, 359 (1977b).
Janardhan, A. S., and G. A. Mansoori, "Fractal Nature of Asphaltene Aggregation," *J. Pet. Sci. Eng.*, **9**, 17 (1993).
Jullien, R., and A. Hasmy, "Fluctuating Bond Aggregation: A Model for Chemical Gel Formation," *Phys. Rev. Lett.*, **74**, 4003 (1995).
Kantor, Y., and T. A. Witten, "Mechanical Stability of Tenuous Objects," *J. Phys. Lett.*, **45**, L-675 (1984).
Kolb, M., R. Botet, and R. Jullien, "Scaling of Kinetically Growing Clusters," *Phys. Rev. Lett.*, **51**, 1123 (1983).
Kyriacou, K. C., R. E. Baltus, and P. Rahimi, "Characterization of Oil Residual Fractions Using Intrinsic Viscosity Measurements," *Fuels*, **67**, 109 (1988a).
Kyriacou, K. C., V. V. Sivaramakrishna, R. E. Baltus, and P. Rahimi, "Measurement of Diffusion Coefficient of Oil Residual Fractions Using Porous Membranes," *Fuels*, **67**, 15 (1988b).
Kuzeev, I. R., I. Z. Mukhametzyanov, and Yu. M. Abyzgil'din, "Macroscopic Structures of Petroleum Pitches in the Course of Solidification," *Kolloid. Zhur.*, **53**, 434 (1991).
Lichaa, P. M., and L. Herrera, "Electrical and Other Effects Related to the Formation and Prevention of Asphaltenes Deposition," *Soc. of Petrol. Engrs., paper 5304* (1975).
Lin, J.-R., H. Lian, K. M. Sadeghi, and T. F. Yen, "Asphalt Colloidal Types Differentiation by Korcak Distribution," *Fuel*, **70**, 1439 (1991).
Liu, Y. C., E. Y. Sheu, S. H. Chen, and D. A. Storm, "Fractal Structure of Asphalt in Toluene," *Fuel*, **74**, 1352 (1995).
Meakin, P., "Formation of Fractal Clusters and Networks by Irreversible Diffusion-Limited Aggregation," *Phys. Rev. Lett.*, **51**, 1119 (1983).
Meakin, P., "The Effect of Rotational Diffusion on the Fractal Dimensionality of Structures Formed by Cluster-Cluster Aggregation," *J. Chem. Phys.*, **81**, 4637 (1984).
Meakin, P., *Phase Transitions and Critical Phenomena*, Vol. 12, C. Domb and J. L. Lebowitz, eds., Academic Press, London (1988).
Meakin, P., T. Vicsek, and F. Family, "Dynamic Cluster-Size Distribution in Cluster-Cluster Aggregation: Effects of Cluster Diffusivity," *Phys. Rev. B.*, **31**, 564 (1985).
Mieville, R. L., D. M. Trauth, and K. K. Robinson, "Asphaltene Characterization and Diffusion Measurements," *ACS Preprints, Div. Pet. Chem.*, **34**, 635 (1989).
Moschopedis, S. E., J. F. Fryer, and J. G. Speight, "Investigation of Asphaltene Molecular Weights," *Fuel*, **55**, 227 (1976).
Moschopedis, S. E., and J. G. Speight, "Investigation of Hydrogen Bonding by Oxygen Functions in Athabasca Bitumen," *Fuel*, **55**, 187 (1976).
Mukhametzyanov, I. Z., and I. R. Kuzeev, "Fractal Structures of Paramagnetic Aggregates of Petroleum Pitches," *Kolloid. Zhur.*, **53**, 644 (1991).
Nortz, R. L., R. E. Baltus, and P. Rahimi, "Determination of the Macroscopic Structure of Heavy Oil by Measuring Hydrodynamic Properties," *Ind. Eng. Chem. Res.*, **29**, 1968 (1990).
Park, S. J., and G. A. Mansoori, "Aggregation and Deposition of Heavy Organics into Petroleum Crudes," *Energy Sources*, **10**, 109 (1988).
Raghunathan, P., "Evidence for Fractal Dimension in Asphalt Polymers from Electron-Spin-Relaxation Measurements," *Chem. Phys. Lett.*, **182**, 331 (1991).
Rassamdana, H., B. Dabir, M. Nematy, M. Farhani, and M. Sahimi, "Asphalt Flocculation and Deposition. I. The Onset of Precipitation," *AIChE J.*, **42**, 10 (1996).
Ravi-Kumar, V. S., T. T. Tsotsis, M. Sahimi, and I. A. Webster, "Studies of Transport of Asphaltenes Through Porous Membranes: Statistical Structural Models and Continuum Hydrodynamic Theories," *Chem. Eng. Sci.*, **49**, 5789 (1994).
Sahimi, M., "Structural and Dynamical Properties of Branched Polymers and Gels and Their Relation with Elastic Percolation Networks," *Mod. Phys. Lett. B*, **6**, 507 (1992).
Sahimi, M., "Flow Phenomena in Rocks: From Continuum Models to Fractals, Percolation, Cellular Automata, and Simulated Annealing," *Rev. Mod. Phys.*, **65**, 1393 (1993).
Sahimi, M., *Applications of Percolation Theory*, Taylor & Francis, London (1994).
Sahimi, M., *Flow and Transport in Porous Media and Fractured Rock*, VCH, Weinheim, Germany (1995).
Sahimi, M., G. R. Gavalas, and T. T. Tsotsis, "Statistical and Continuum Models of Fluid-Solid Reactions in Porous Media," *Chem. Eng. Sci.*, **45**, 1443 (1990).
Sakai, M., K. Sasaki, and M. Inagaki, "Hydrodynamic Studies of Dilute Pitch Solutions: The Shape and Size of Pitch Molecules," *Carbon*, **21**, 593 (1983).
Sane, R. C., I. A. Webster, and T. T. Tsotsis, "Study of Asphaltene Diffusion Through Unimodal Porous Membrane," *Studies Surf. Sci. Catal.*, **38**, 705 (1988).
Sane, R. C., I. A. Webster, T. T. Tsotsis, and V. S. Ravi-Kumar, *Asphalts and Asphaltenes*, T. F. Yen, ed., Elsevier, New York (1992).
Savage, P. E., and M. T. Klein, "Asphaltene Reaction Pathways—V. Chemical and Mathematical Modeling," *Chem. Eng. Sci.*, **44**, 393 (1989).
Schaefer, D. W., J. E. Martin, P. Wiltzuis, and D. S. Cannel, "Fractal Geometry of Colloidal Aggregates," *Phys. Rev. Lett.*, **52**, 2371 (1984).
Schwager, I., and T. F. Yen, "Coal-Liquefaction Products from Major Demonstration Processes. 1. Separation and Analysis," *Fuel*, **57**, 100 (1978).
Sheu, E. Y., K. S. Liang, S. K. Sinha, and R. E. Overfield, "Polydispersity Analysis of Asphaltene Solutions in Toluene," *J. Colloid Interf. Sci.*, **153**, 399 (1992).
Snape, C. E., and K. D. Bartle, "Definition of Fossil Fuel-Derived Asphaltenes in Terms of Average Structural Properties," *Fuel*, **63**, 883 (1984).
Speight, J. G., *The Chemistry and Technology of Petroleum*, Dekker, New York (1991).
Speight, J. G., and S. E. Moschopedis, "Asphaltene Molecular Weights by a Cryoscopic Method," *Fuel*, **56**, 344 (1977).
Speight, J. G., and S. E. Moschopedis, "On the Polymeric Nature of Petroleum Asphaltenes," *Fuel*, **59**, 440 (1980).
Speight, J. G., D. L. Wernick, K. A. Gould, R. E. Overfield, B. M. L. Rao, and D. W. Savage, "Molecular Weight and Association of Asphaltenes: A Critical Review," *Rev. Inst. Fr. Pet.*, **40**, 52 (1985).
Storm, D. A., E. Y. Sheu, and M. DeTar, "Macrostructure of Asphaltenes in Vacuum Residue by Small-Angle X-Ray Scattering," *Fuel*, **72**, 977 (1993).
Strausz, O. P., T. W. Mojelsky, and E. M. Lown, "The Molecular Structure of Asphaltene: An Unfolding Story," *Fuel*, **71**, 1355 (1992).
Taylor, S. E., "Use of Surface Tension Measurements to Evaluate Aggregation of Asphaltenes in Organic Solvents," *Fuel*, **71**, 1338 (1992).
Thrash, R. J., and R. H. Pildes, "The Diffusion of Petroleum Asphaltenes Through Well Characterized Porous Membranes," *ACS Preprints, Div. Pet. Chem.*, **26**, 515 (1981).
Toulhoat, H., C. Prayer, and G. Rouquet, "Characterization by Atomic Force Microscopy of Adsorbed Asphaltenes," *Colloids Surf.*, **91**, 267 (1994).
Trauth, D. M., S. M. Stark, T. F. Petti, M. Neurock, and M. T. Klein, "Representation of the Molecular Structure of Petroleum Resid through Characterization and Monte Carlo Modeling," *Energy & Fuels*, **8**, 576 (1994).
Vicsek, T., and F. Family, "Dynamic Scaling for Aggregation of Clusters," *Phys. Rev. Lett.*, **52**, 1669 (1984).
Witten, T. A., and L. M. Sander, "Diffusion-Limited Aggregation, a Kinetic Critical Phenomenon," *Phys. Rev. Lett.*, **47**, 1400 (1981).
Yen, T. F., "Structure of Petroleum Asphaltene and its Significance," *Energy Sources*, **1**, 447 (1974).
Yen, T. F., *Encyclopedia of Polymer Science and Engineering*, 2nd ed., H. F. Mark, N. M. Bikales, C. G. Overberger, and G. Menges, eds., Wiley, New York, p. 1 (1990).
Ziff, R. M., E. D. McGrady, and P. Meakin, "On the Validity of Smoluchowski's Equation for Cluster-Cluster Aggregation Kinetics," *J. Chem. Phys.*, **82**, 5269 (1985).

Manuscript received June 19, 1995, and revision received May 13, 1996.